AD-A035 902 SYRACUSE UNIV N Y DEPT OF ELECTRICAL AND COMPUTER E--ETC F/G 9/5
A SOLUTION FOR A WIDE APERTURE REACTIVELY LOADED ANTENNA ARRAY.(U)
JAN 77 J LUZWICK, R F HARRINGTON N00014-76-C-0225

UNCLASSIFIED TR-77-1 NL

1 OF 1
ADA035902

END

DATE
FILMED
3-77

UNCLASSIFIED

SECURITY CLASSIFICATION OF THIS PAGE (When Data Entered)

REPORT DOCUMENTATION PAGE	READ INSTRUCTIONS BEFORE COMPLETING FORM
1. REPORT NUMBER (14) TR-77-1, TR-5	2. GOVT ACCESSION NO.
3. RECIPIENT'S CATALOG NUMBER	
4. TITLE (and Subtitle) (6) A SOLUTION FOR A WIDE APERTURE REACTIVELY LOADED ANTENNA ARRAY.	5. TYPE OF REPORT & PERIOD COVERED (9) Technical Report, No. 5
6. PERFORMING ORG. REPORT NUMBER	
7. AUTHOR(s) (10) John Luzwick, Roger F. Harrington	8. CONTRACT OR GRANT NUMBER(s) (15) N00014-76-C-0225
9. PERFORMING ORGANIZATION NAME AND ADDRESS Dept. of Electrical and Computer Engineering, Syracuse University, Syracuse, New York 13210	10. PROGRAM ELEMENT, PROJECT, TASK AREA & WORK UNIT NUMBERS
11. CONTROLLING OFFICE NAME AND ADDRESS Department of the Navy, Office of Naval Research, Arlington, Virginia 22217	(11) 12. REPORT DATE January 1977; 13. NUMBER OF PAGES 30
14. MONITORING AGENCY NAME & ADDRESS (if different from Controlling Office) (12) 31 p.	15. SECURITY CLASS. (of this report) UNCLASSIFIED; 15a. DECLASSIFICATION/DOWNGRADING SCHEDULE

16. DISTRIBUTION STATEMENT (of this Report)

Approved for public release; distribution unlimited

17. DISTRIBUTION STATEMENT (of the abstract entered in Block 20, if different from Report)

18. SUPPLEMENTARY NOTES

19. KEY WORDS (Continue on reverse side if necessary and identify by block number)

Aperture antennas
Aperture arrays
Computer programs
Reactive loads
Waveguide-backed apertures
Wide apertures

20. ABSTRACT (Continue on reverse side if necessary and identify by block number)

This report considers an array of wide aperture reactively loaded antennas, specifically, an N element array of closely-spaced waveguide-backed rectangular slots radiating into a half-space region. Only the center slot is fed and the other slots are parasitically excited. The parasitic slots are reactively loaded by short-circuit waveguides. By varying the positions of the short circuits, a directive beam can be steered through 180° in space. The solution uses the moment method applied to the integral equation for the equi-

DD FORM 1 JAN 73 1473 EDITION OF 1 NOV 65 IS OBSOLETE S/N 0102-014-6601

UNCLASSIFIED

SECURITY CLASSIFICATION OF THIS PAGE (When Data Entered)

406 737

valent magnetic current in the aperture region and a numerical integration technique. Solutions for seven, nine, and fifteen element aperture arrays are given. A computer subroutine which generates the aperture half-space admittance matrix is described and listed.

CONTENTS

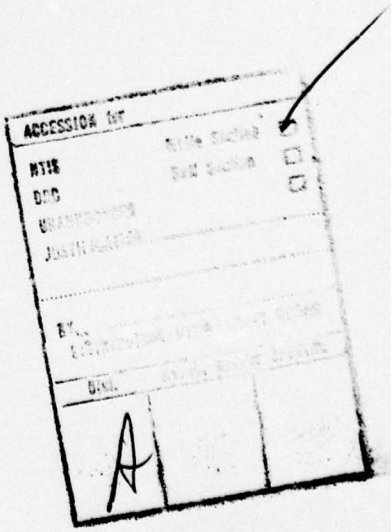

PART ONE

THEORY AND EXAMPLES

I. INTRODUCTION

In a previous report [1] it was demonstrated that for a reactively-loaded waveguide-fed aperture antenna array the radiation characteristics can be controlled by feeding one aperture and reactively loading the other apertures. The reactive loads can be realized by placing electrical short circuits in the unfed waveguides at variable distances from the apertures. By varying these short circuit positions, the antenna beam can be steered.

The use of thin apertures with waveguides of the same cross sectional dimensions resulted in a sizable mismatch between the wave admittance and the half-space admittance at the aperture boundary. This resulted in small reactive load magnitudes (referenced to the wave admittance) and small changes in short circuit distances per degree change in antenna beam position. It also necessitated the use of non-standard waveguide. In this report a wide aperture antenna array is analyzed. The above mentioned problem areas are reduced by changing from thin to wide apertures.

The aperture antenna array studied consists of closely spaced apertures which allow large mutual coupling to exist between apertures. Each aperture, therefore, has a large effect on the resultant antenna beam shape and position.

II. STATEMENT OF THE PROBLEM

Figure 1 illustrates a seven element waveguide-fed dielectric-filled rectangular aperture array. The following assumptions are made:

1. A perfectly conducting plate covers the entire $z = 0$ plane except for the apertures.
2. The apertures are one-half wavelength long.
3. The dominant mode is assumed to be the only mode present in each waveguide (all other modes are cut-off).

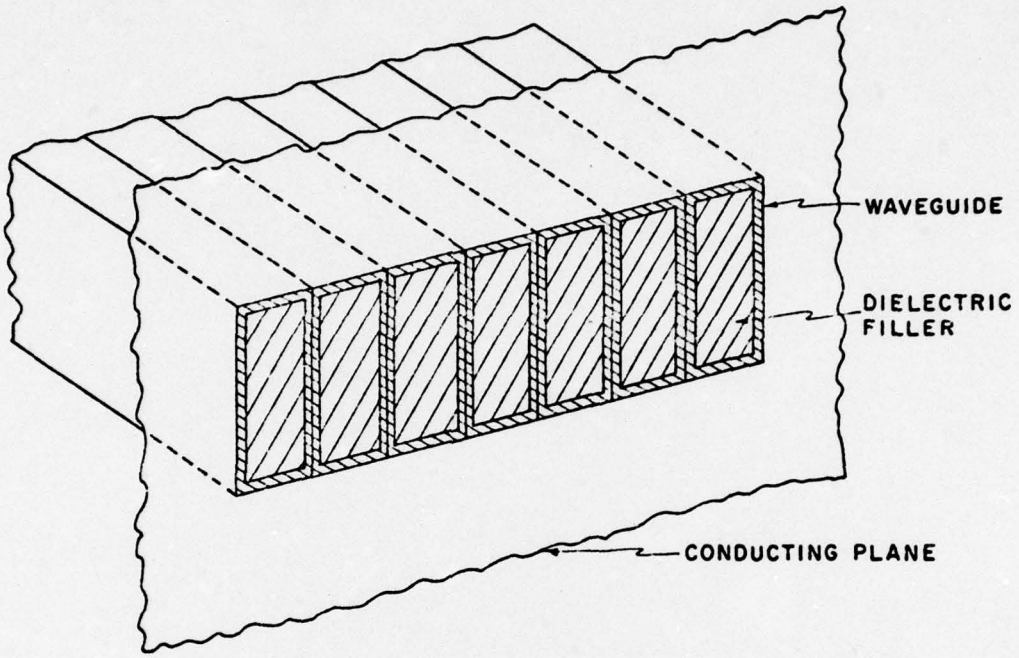

Fig. 1. An array of waveguide-backed dielectric-filled apertures radiating into half-space bounded by an electric conductor.

4. The waveguide dielectric filler lowers the cut-off frequency for the dominant mode so that the assumption of a cosine tangential electric field existing across each aperture is reasonable.

The general method of solution [2] is to cover the K apertures with a perfect conductor, to place magnetic current sheets $+\underset{\sim}{M}^j$ and $-\underset{\sim}{M}^j$, respectively, on the left-hand and right-hand sides of the conductor, to obtain an integral equation for each $\underset{\sim}{M}^j$ (j = 1,2,...,K) by equating the tangential magnetic fields on both sides of the conductor, and to solve these integral equations using the method of moments. The testing functions are the same as the expansion functions $\underset{\sim}{M}_j$. Each $\underset{\sim}{M}_j$ is a cosine function in the direction of current and a pulse function in the direction perpendicular to the current. For our problem the current is in the y direction only.

III. SUMMARY OF BASIC THEORY

The orientation of the apertures and the coordinate system is shown in Fig. 2. The equivalent magnetic current in the jth aperture region is represented by

$$\underset{\sim}{M}^j = V_j \, \underset{\sim}{M}_j \tag{1}$$

where the V_j are constants to be determined. The solution given by [1] is

$$\vec{V} = [Y^{wg} + Y^{hs}]^{-1} \vec{I}^i \tag{2}$$

where $\vec{V}$ is the column vector of the V_j. The magnetic current expansion function in the jth aperture is taken to be

$$M_j = P_j(x) \cos ky \ . \tag{3}$$

In (2) the diagonal matrix $[Y^{wg}]$ is generated by two distinct expressions:

a) For $i = \frac{K+1}{2}$ (K is the number of apertures),

$$Y^{wg}_{ii} = [\frac{2}{wL} < -\cos ky, \quad H^{wg}_{t_{ii}} (\cos ky) >]$$

$$= Y_o \text{ (dominant mode wave admittance)} \tag{4}$$

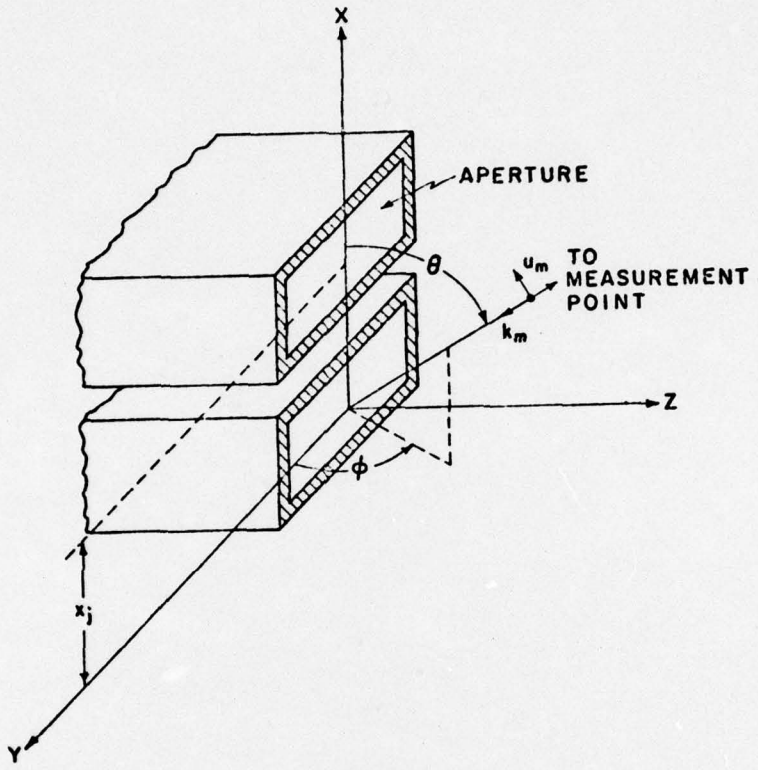

Fig. 2. Orientation of the apertures and the coordinate system.

(Note: < > is the mathematical symbol for symmetric product

$$\langle A,B\rangle = \iint_{\text{surface}} \underset{\sim}{A} \cdot \underset{\sim}{B}\, dS.)$$

b) For $i \neq \frac{K+1}{2}$,

$$Y^{wg}_{ii} = [\frac{2}{wL} \langle - \cos ky,\ H^{wg}_{t_{ii}} (\cos ky)\rangle]$$

$$= - j\, Y_o \cot k_1 d^i(\theta) \qquad (5)$$

where $d^i(\theta)$ is the distance of the short circuit from the aperture in the ith waveguide (dependent on beam steering angle θ)

k is the free-space wave number

k_c is the cut-off wave number

$k_1 = \sqrt{\varepsilon_r k^2 - k_c^2}$

ε_r is the relative permittivity of the dielectric filler

η is the free-space intrinsic impedance

$$Y_o = \frac{1}{\eta} \sqrt{\varepsilon_r - (k_c/k)^2}\ .$$

In (2) the matrix $[Y^{hs}]$ is given by

$$Y^{hs}_{ij} = \iint_{\text{aperture}} - \underset{\sim}{M}_i \cdot \underset{\sim}{H}^{hs}_{t_{ij}} (\underset{\sim}{M}_j) dS \qquad (6)$$

where $\underset{\sim}{H}^{hs}_{t_{ij}} (\underset{\sim}{M}_j)$ is the tangential magnetic field in the ith aperture generated by the equivalent magnetic current in the jth aperture. In (2) the column vector $\vec{I}^i$ consists of one non-zero element which corresponds to the excitation (externally driven waveguide). In (3) the expression $P_j(x)$ is given by

$$P_j(x) = \begin{cases} \frac{2}{wL}, & x_j - \frac{w}{2} \leq x \leq x_j + \frac{w}{2} \quad \text{(see Fig. 2)} \\ 0, & \text{all other } x. \end{cases}$$

The gain (ratio of the maximum radiation intensity in a given direction to the maximum radiation produced in the same direction from an isotropic radiator with the same power input) corresponding to the direction (θ,ϕ) in the half-space $z > 0$ is given by (* means complex conjugate)

$$G(\theta,\phi) = \frac{k^2}{8\pi\eta \text{ Real } (\tilde{V}[Y^{hs}]^* \vec{V}^*)} \left|\tilde{P}^m(\theta,\phi)\vec{V}\right|^2 \tag{7}$$

where

$$P_j^m(\theta,\phi) = 2 \iint_{\substack{j\text{th} \\ \text{aperture}}} M_j \, \underset{\sim}{u}_y \cdot \underset{\sim}{u}_m \, e^{-jk_{\sim m} \cdot \underset{\sim}{r}} \, dS \tag{8}$$

(Note: $\tilde{P}^m(\theta,\phi)$ represents a vector of short circuit currents when the array is excited by a plane wave from the direction (θ,ϕ). $\tilde{P}^m(\theta,\phi)$ can be polarized in the θ or ϕ direction.) For the set of all $\tilde{P}^m(\theta,\phi)$ vectors in the E-plane $(0 \leq \theta \leq 180°, \ \phi = 90°)$ and y-polarized, we have

$$P_{yj}^m \text{ (E-plane)} = P_{yj}^m \left(\theta, \frac{\pi}{2}\right)$$

$$= \frac{-4\sqrt{2}}{k} \sqrt{\frac{w}{L}} \, e^{jkx_j \cos\theta} \left(\frac{\sin\left(\frac{kw}{2} \cos\theta\right)}{\frac{kw}{2} \cos\theta} \right) \tag{9}$$

IV. HALF-SPACE ADMITTANCE MATRIX $[Y^{hs}]$ DETERMINATION

In this section the application of a numerical integration technique to determine the half-space admittance for a wide aperture is presented. The procedure followed is to first subdivide the equivalent magnetic current sheet over each aperture region into p current strips (see Fig. 3). By using these current strips as sources, the self and mutual admittances of these sub-aperture regions are found by using previously derived formulas for the thin aperture case [1]. Finally, these

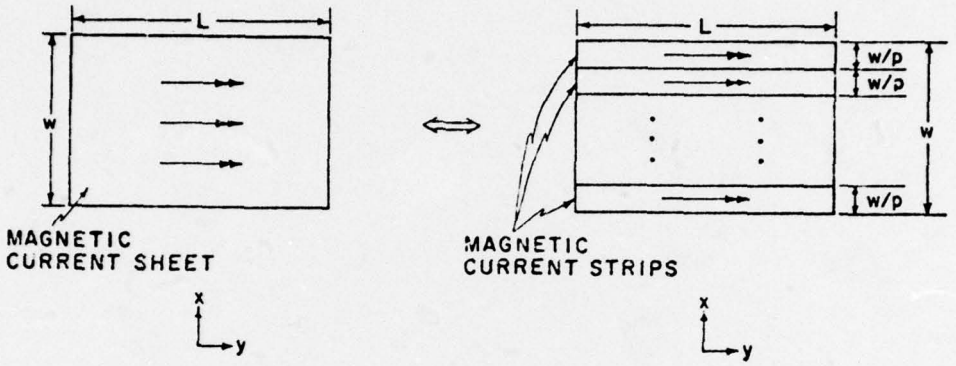

Fig. 3. Subdivision of a magnetic current sheet into p equal magnetic current strips.

individual admittances for the sub-aperture regions (both self and mutual) are summed to yield a single self admittance term for the entire aperture. This technique is then extended to include the mutual admittance terms between all of the aperture of the array. We first consider the single aperture case and then extend the results to that of the multiple aperture array.

In the preceding section, the half-space admittance for a single aperture was defined to be

$$Y^{hs} = \iint_{\text{aperture}} - \underset{\sim}{M} \cdot \underset{\sim}{H}_t^{hs}(\underset{\sim}{M})\, dS \tag{10}$$

where

$$\underset{\sim}{M} = \underset{\sim}{u}_y \sqrt{\frac{2}{wL}} \cos ky, \tag{11}$$

$$-\frac{w}{2} \leq x \leq \frac{w}{2}.$$

Let

$$\underset{\sim}{M} = \sum_{q=1}^{p} \underset{\sim}{M}_q \quad \text{(see Fig. 3)} \tag{12}$$

where

$$\underset{\sim}{M}_q = \underset{\sim}{u}_y \sqrt{\frac{2}{wL}} \cos ky\ , \tag{13}$$

$$-\frac{w}{2} + (q-1)\frac{w}{p} \leq x \leq -\frac{w}{2} + (q)\frac{w}{p}$$

$$q = 1,2,\ldots, p.$$

Then

$$Y^{hs} = -2 \sum_{q=1}^{p} \sum_{r=1}^{p} \int_{-L/2}^{L/2} dy \int_{-w/2+(q-1)w/p}^{-w/2+(q)w/p} dx\, \underset{\sim}{M}_q \cdot \underset{\sim}{H}_t(\underset{\sim}{M}_r) \tag{14}$$

where the factor 2 is due to image theory. (The magnetic current expansion function $\underset{\sim}{M}_q$ is on the surface of the $z=0$ plane which is now a complete conducting plane since the aperture is covered by a conductor - Y^{hs} is the admittance obtained using expansion functions $2\,\underset{\sim}{M}_q$ radiating

into free space everywhere.) $\underset{\sim}{H}_t(\underset{\sim}{M}_r)$ is the tangential magnetic field due to $\underset{\sim}{M}_r$ radiating into free space. $\underset{\sim}{M}_q$ is approximated by a filament $\underset{\sim}{u}_y\sqrt{\frac{2}{wL}}\,(\frac{w}{p})\cos ky$ of magnetic current at $x = \frac{-w}{2} + (q - 0.5)\,\frac{w}{p}$. By substituting this approximation for $\underset{\sim}{M}_q$ and a similar approximation for $\underset{\sim}{M}_r$ into (14), we obtain

$$Y^{hs} = -\,2\,(\frac{2}{wL})\,(\frac{w}{p})^2 \sum_{q=1}^{p}\sum_{r=1}^{p} \int_{-L/2}^{L/2} dy\; \underset{\sim}{u}_y \cos ky \cdot \underset{\sim}{H}_{t_{qr}} \tag{15}$$

where $\underset{\sim}{H}_{t_{qr}}$ is the tangential magnetic field due to the filament $\underset{\sim}{u}_y \cos ky$ of magnetic current at $x = \frac{-w}{2} + (r - 0.5)\,\frac{w}{p}$ evaluated at $x = \frac{-w}{2} + (q - 0.5)\frac{w}{p}$.

To solve (15), we substitute an equivalent expression for $\underset{\sim}{H}_{t_{qr}}$ for which the resultant integral has a known solution. This expression can be derived as follows. For a source free region,

$$\underset{\sim}{\nabla} \times \underset{\sim}{E} = -\,j\omega\mu\,\underset{\sim}{H} \tag{16}$$

$$\underset{\sim}{\nabla} \times \underset{\sim}{H} = j\omega\varepsilon\,\underset{\sim}{E} \tag{17}$$

Let

$$\underset{\sim}{E} = -\,\underset{\sim}{\nabla} \times \underset{\sim}{F} \tag{18}$$

and

$$\underset{\sim}{H} = \underset{\sim}{\nabla} \times \underset{\sim}{A} \tag{19}$$

where

$$\underset{\sim}{F}(\underset{\sim}{r}) = \frac{1}{4\pi} \iiint \frac{\underset{\sim}{M}(\underset{\sim}{r}')\; e^{-jk|\underset{\sim}{r}-\underset{\sim}{r}'|}}{|\underset{\sim}{r} - \underset{\sim}{r}'|}\, d\tau' \tag{20}$$

$$\underset{\sim}{A}(\underset{\sim}{r}) = \frac{1}{4\pi} \iiint \frac{\underset{\sim}{J}(\underset{\sim}{r}')\; e^{-jk|\underset{\sim}{r}-\underset{\sim}{r}'|}}{|\underset{\sim}{r} - \underset{\sim}{r}'|}\, d\tau' \;. \tag{21}$$

By substituting (18) into (16) and (19) into (17), we obtain

$$\underset{\sim}{H} = \frac{1}{j\omega\mu} \underset{\sim}{\nabla} \times \underset{\sim}{\nabla} \times \underset{\sim}{F} \tag{22}$$

$$\underset{\sim}{E} = \frac{1}{j\omega\mu} \underset{\sim}{\nabla} \times \underset{\sim}{\nabla} \times \underset{\sim}{A} \, . \tag{23}$$

Therefore, $\underset{\sim}{H}$ due to $\underset{\sim}{M}$ is $\frac{1}{\eta^2}$ times $\underset{\sim}{E}$ due to $\underset{\sim}{J}$. Using this relationship, (15) transforms to

$$Y^{hs} = \left(\frac{4}{\eta^2}\right)\left(\frac{w}{L}\right)\left(\frac{1}{p^2}\right) \sum_{q=1}^{p} \sum_{r=1}^{p} \left[- \int_{-L/2}^{L/2} dy \, \underset{\sim}{u}_y \cos ky \cdot \underset{\sim}{E}_{t_{qr}} \right. \tag{24}$$

where $\underset{\sim}{E}_{t_{qr}}$ is the tangential electric field due to a filament $\underset{\sim}{u}_y \cos ky$ of electric current at $x = -\frac{w}{2} + (r - 0.5)\frac{w}{p}$ evaluated at $x = -\frac{w}{2} + (q - 0.5)\frac{w}{p}$.

For the self admittance terms (q=r), we separate the field and source filaments by a distance $(\frac{w}{p})/4$ which is the "equivalent radius" for a rectangular strip. The quantity in brackets in (24) represents the self and mutual impedances of thin dipoles in an array. Therefore, (24) can be written as

$$Y^{hs} = \left(\frac{4}{\eta^2}\right)\left(\frac{w}{L}\right)\left(\frac{1}{p^2}\right) \sum_{q=1}^{p} \sum_{r=1}^{p} Z_{qr} \, . \tag{25}$$

To extend this development to the multiple aperture case, (10) can be rewritten as

$$Y^{hs}_{ij} = \iint_{\text{aperture}} - \underset{\sim}{M}_i \cdot \underset{\sim}{H}^{hs}_{t_{ij}} (\underset{\sim}{M}_j) \, dS \, . \tag{26}$$

Y^{hs}_{ij} $(i \neq j)$ represents the mutual admittance between the ith and jth apertures while Y^{hs}_{ij} $(i = j)$ represents the self admittance of the ith (jth) aperture. $\underset{\sim}{H}^{hs}_{t_{ij}} (\underset{\sim}{M}_j)$ represents the tangential magnetic field in the ith aperture generated by the equivalent magnetic current sheet in the jth aperture.

Let

$$\underset{\sim}{M}_i = \sum_{q=1}^{p} \underset{\sim}{M}_{iq} = \underset{\sim}{u}_y \sqrt{\frac{2}{wL}} \cos ky, \qquad (27)$$

$$-\frac{w}{2} + x_i \leq x \leq \frac{w}{2} + x_i$$

(x_i is the distance from the origin to the center of the ith aperture.)
where

$$\underset{\sim}{M}_{iq} = \underset{\sim}{u}_y \sqrt{\frac{2}{wL}} \cos ky, \qquad (28)$$

$$-\frac{w}{2} + x_i + (q-1)\frac{w}{p} \leq x \leq -\frac{w}{2} + x_i + q\frac{w}{p}$$

$$q = 1,2,\ldots, p.$$

Substituting (27) into (26) we obtain

$$Y_{ij}^{hs} = -2 \sum_{q=1}^{p} \sum_{r=1}^{p} \int_{-\frac{L}{2}}^{\frac{L}{2}} dy \int_{\frac{-w}{2} + x_i + (q-1)\frac{w}{p}}^{\frac{-w}{2} + x_i + q\frac{w}{p}} dx \, \underset{\sim}{M}_{iq} \cdot \underset{\sim}{H}_{t(iq)(jr)}$$

$$= \left(\frac{4}{\eta^2}\right)\left(\frac{w}{L}\right)\left(\frac{1}{p^2}\right) \sum_{q=1}^{p} \sum_{r=1}^{p} \left(- \int_{\frac{-L}{2}}^{\frac{L}{2}} dy \, \underset{\sim}{u}_y \cos ky \cdot \underset{\sim}{E}_{t(iq)(jr)} \right)$$

$$= \left(\frac{4}{\eta^2}\right)\left(\frac{w}{L}\right)\left(\frac{1}{p^2}\right) \sum_{q=1}^{p} \sum_{r=1}^{p} Z_{(iq)(jr)} \qquad (29)$$

where $Z_{(iq)(jr)}$ $(i \neq j)$ represents the mutual impedance between the (iq)th and (jr)th dipole current filaments.

V. REPRESENTATIVE COMPUTATIONS

A computer program using the preceding formulas has been written and is included in report [1] with the exception of YHSPA (generates the half-space admittance matrix for a wide aperture array using a numerical integration technique) which is included in Part Two of this report. For this section results will be given for N = 7, 9, and 15 element aperture arrays. In all of the cases to be presented, the aperture width is 0.25λ and six magnetic current strips are used per aperture region. The initial reactive loads required for the optimization subroutine are the reactive loads which resonate complex equivalent sources. All of the gain patterns are taken in the E-plane ($0 \leq \theta \leq 180°$, $\phi = 90°$).

Figures 4 and 5 illustrate the maximum gain that can be obtained for a seven element aperture array using a single feed and reactively loading the other apertures. The triangular symbols Δ in the two figures represent the maximum gain that can be obtained for the same aperture antenna by feeding each aperture with the optimum complex equivalent voltage. It should be noted that both excitations yield excessively large beamwidths at low angles ($0 \leq \theta \leq 40°$).

Figure 6 represents the same case of a seven element aperture array considered in Figures 4 and 5 (for $\theta = 0$, 30°, 60°, and 90°), with a 1% loss factor added. In addition to the loss of gain in the desired directions, the backlobe in the $\theta = 0$ pattern is greatly reduced.

Figure 7 illustrates the maximum gain that can be obtained for a nine element aperture array using a single feed and reactively loading the other apertures. A general increase in gain is observed with no apparent change in the sidelobe structure compared to the seven element aperture array case.

Figure 8 illustrates the maximum gain that can be obtained for a fifteen element aperture array using a single feed and reactive loading the other apertures, with a 0.1% loss factor added. Relative sidelobe levels at $\theta = 60°$, 75°, and 90° have decreased in comparison to the seven and nine element aperture arrays.

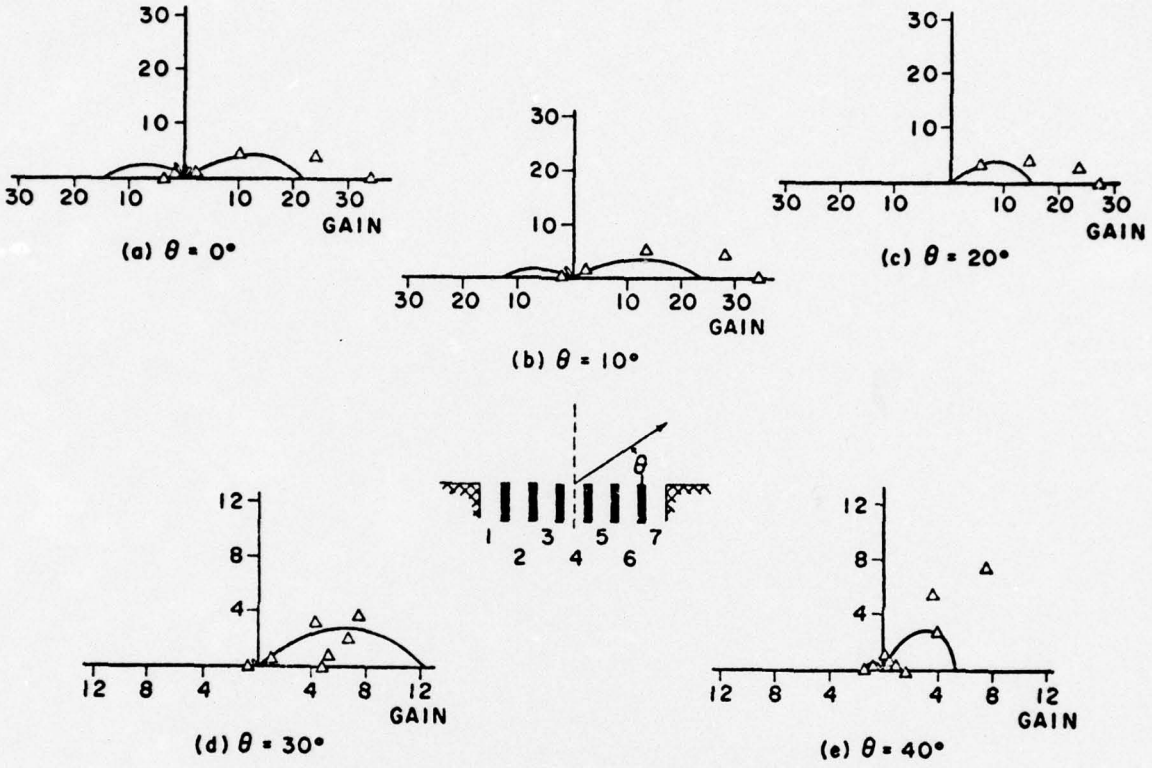

Fig. 4. Radiation gain patterns for a seven element aperture array. The solid lines represent the pattern for the reactively loaded array with only the center element fed. The triangles represent the pattern for the array when all elements are fed with the excitation for maximum gain. Aperture width is 0.25λ. Six current strips per aperture were used to evaluate the admittance elements.

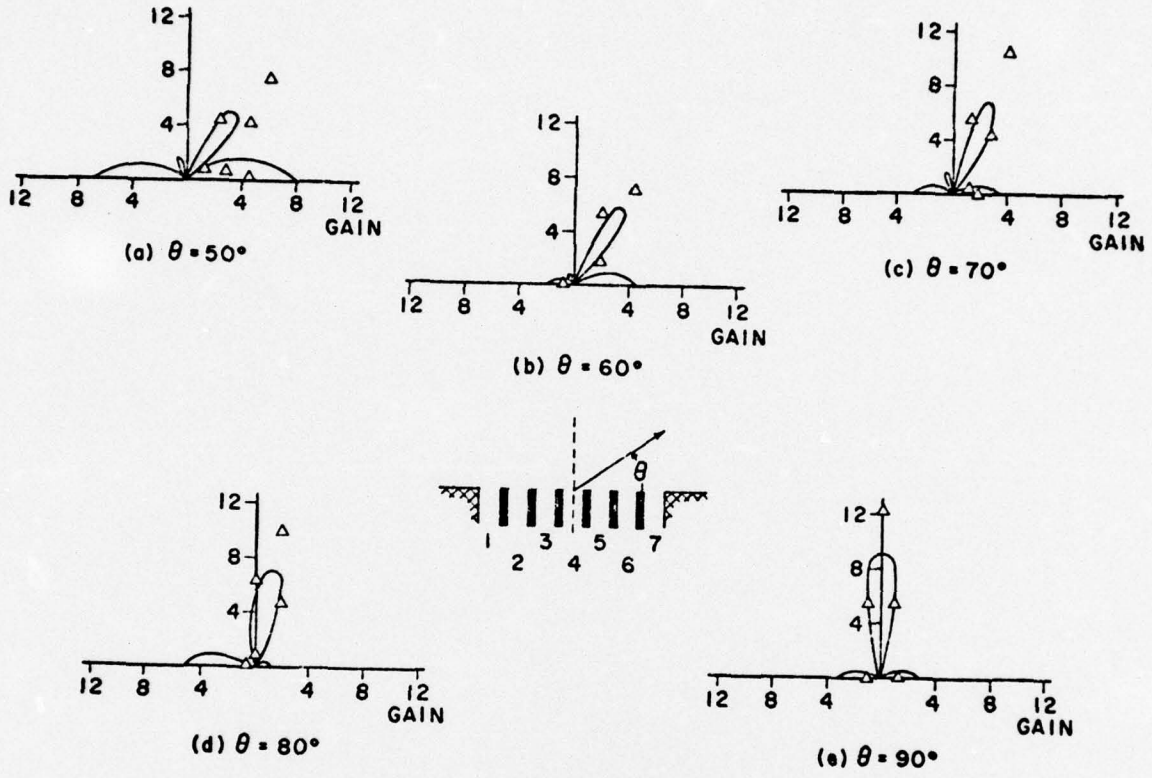

Fig. 5. Radiation gain patterns for a seven element aperture array. The solid lines represent the pattern for the reactively loaded array with only the center element fed. The triangles represent the pattern for the array when all elements are fed with the excitation for maximum gain. Aperture width is 0.25λ. Six current strips per aperture were used to evaluate the admittance elements.

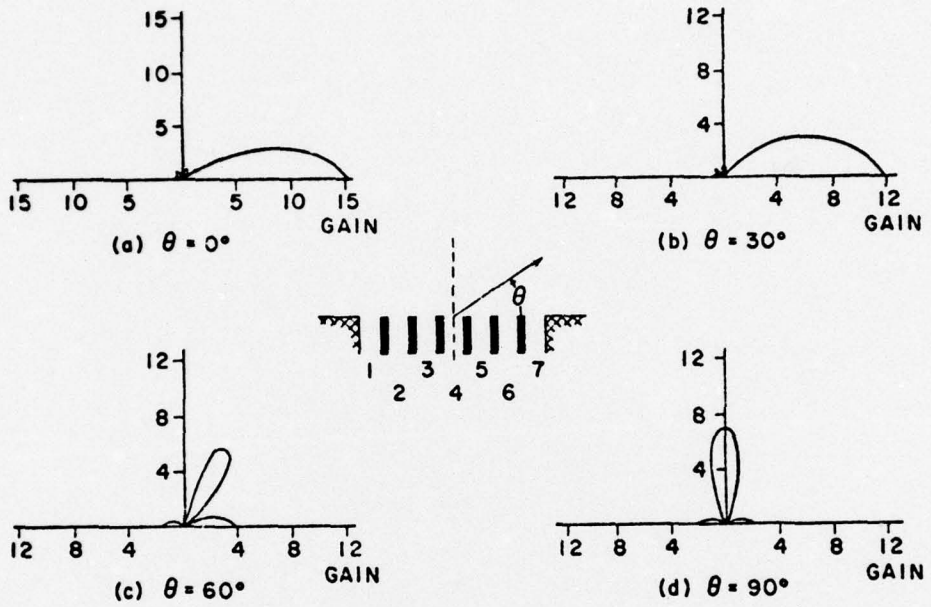

Fig. 6. Radiation gain patterns for a seven element reactively loaded aperture array with only the center element fed. Aperture width is 0.25λ. Six current strips per aperture were used to evaluate the admittance elements. A loss factor of 0.1% was added to the real parts of the diagonal admittance elements.

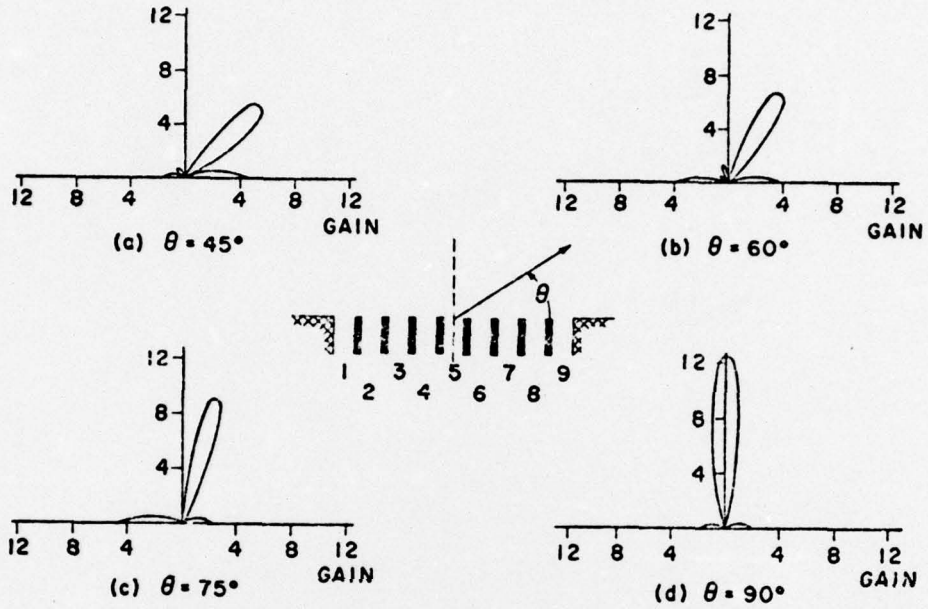

Fig. 7. Radiation gain patterns for a nine element reactively loaded aperture antenna with only the center element fed. Aperture width is 0.25λ. Six current strips per aperture were used to evaluate the admittance elements.

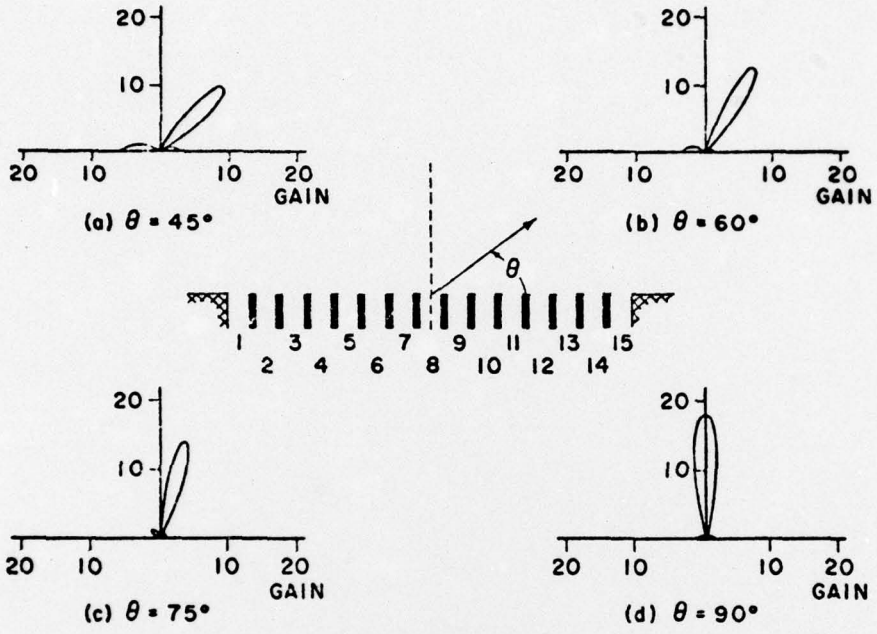

Fig. 8. Radiation gain patterns for a fifteen element reactively loaded aperture array with only the center element fed. Aperture width is 0.25λ. Six current strips per aperture were used to evaluate the admittance elements. A loss factor of 0.1% was added to the real parts of the diagonal admittance elements.

Table 1 lists the reactive load values required to steer the beam from 0 to 90° in 10° steps for the seven element lossless aperture array (see Figs. 4 and 5). (Note that both inductive and capacitive reactances are required.)

Table 2 lists the reactive load values and equivalent short circuit distances required for a nine element lossless array (see Fig. 7). The distance magnitudes are referenced to WR-75 (2.159 cm x 1.206 cm -- wall thickness 0.127 cm) filled with a dielectric $\varepsilon_r = 1.55$ and operating at a frequency of 7.88 GHz. Admittedly, if larger waveguide and a lower operating frequency were chosen, the changes in short circuit distances required for beam steering would be larger. The choice of WR-75 and a frequency of 7.88 GHz was made to illustrate that very small changes in electrical short positions are required to steer the beam in increments of 15° for waveguides of these relative dimensions and operating frequencies at or above 7.88 GHz.

Table 1. Reactive load values (mmhos) for a seven element aperture array using six strips per aperture region and w = 0.25λ (see Figs. 4 and 5).

Aperture No.	θ = 0°	θ = 10°	θ = 20°	θ = 30°
1	+ 0.102 m℧	+ 0.114 m℧	+ 27.9 m℧	- 1.20 m℧
2	- 0.371	- 0.363	- 0.109	+ 0.335
3	- 0.583	- 0.584	- 0.424	- 0.351
5	- 0.648	- 0.659	- 0.810	- 0.981
6	- 0.440	- 0.418	- 0.855	- 1.40
7	+ 0.339	+ 0.571	- 2.50	- 7.26

Aperture No.	θ = 40°	θ = 50°	θ = 60°	θ = 70°
1	- 0.307 m℧	- 2.18 m℧	- 0.079 m℧	+ 0.085 m℧
2	- 3.33	+ 0.195	- 1.68	- 0.831
3	- 0.068	- 0.516	- 0.036	- 0.438
5	- 1.30	- 0.567	- 0.959	- 0.793
6	- 4.63	- 0.419	- 0.260	- 0.155
7	+ 6.93	- 0.540	- 0.534	- 0.688

Aperture No.	θ = 80°	θ = 90°
1	+ 0.036 m℧	+ 0.197 m℧
2	- 1.20	- 0.754
3	- 0.358	- 0.412
5	+ 0.152	- 0.412
6	- 0.491	- 0.754
7	- 4.82	+ 0.197

Table 2. Reactive load value (B_{Load}) and short circuit distances ($d^i(\theta)$) for a nine element aperture array using six strips per aperture region, waveguide WR-75 (2.159 cm x 1.206 cm - wall thickness 0.127 cm), W = 0.25λ, ε_r = 1.55, and frequency = 7.88 GHz (see Fig. 7).

Aperture No.	θ = 45°		θ = 60°	
	B_{Load}	$d^i(\theta)$*	B_{Load}	$d^i(\theta)$
1	+0.070 m℧	26.041 mm	-1.992 m℧	6.392 mm
2	-1.56	7.381	+0.219	26.658
3	+0.137	26.319	-0.457	11.007
4	-0.410	11.193	-0.584	10.513
6	-0.658	10.233	-0.637	10.312
7	-0.429	11.118	-0.578	10.536
8	-0.453	11.023	-0.279	11.722
9	-0.749	9.898	-0.306	11.612

Aperture No.	θ = 75°		θ = 90°	
	B_{Load}	$d^i(\theta)$	B_{Load}	$d^i(\theta)$
1	+0.146 m℧	26.356 mm	+0.181 m℧	26.501 mm
2	-0.456	11.011	-0.468	10.964
3	-0.457	11.007	-0.422	11.146
4	-0.575	10.548	-0.617	10.388
6	-0.521	10.756	-0.617	10.388
7	-0.459	10.648	-0.422	11.146
8	-0.207	12.018	-0.468	10.964
9	-0.209	12.009	+0.181	26.501

* Distances are measured from the aperture interface or a multiple of one-half wavelength from the aperture plus the given short circuit distance.

VI. DISCUSSION AND CONCLUSIONS

It was found that, for lossless aperture arrays consisting of eleven elements or less, the equivalent magnetic current sheet should be subdivided into three magnetic current strips for an aperture width of 0.10λ, and six magnetic current strips for an aperture width of 0.30λ. The criteria used was the change in magnitude of aperture half-space admittance terms as the number of strips was changed, and whether or not a positive definite Real (Y^{hs}) matrix resulted. When the number of apertures increased beyond eleven, the number of required subdivisions was not easy to predict for the lossless case. For instance, for a fifteen element lossless aperture array, 30 subdivisions were required before a positive definite matrix Real(Y^{hs}) was realized. In addition, using this [Y^{hs}] matrix in an optimization subroutine proved to be costly in computer (CPU) time, due to slow convergence.

Adding loss for aperture arrays consisting of eleven elements or more appears to be the best compromise between the maximum gain values realized and minimum computer (CPU) time required for optimization (Fig. 8 is an example). The use of the number of subdivisions required for a given aperture width for an eleven element or less lossless aperture array proved also to be satisfactory for a lossy aperture array with elements numbering greater than eleven.

From Figs. 4 and 5 it was observed that the beamwidth was large at the low beam steering angles. This observation was true both for the case of complex excitation (all elements fed) and for the case of single waveguide excitation and reactive loading. One method of producing a narrower beam at low beam steering angles is to place a dielectric slab over the apertures. The function of the dielectric slab is to transform the emanating electromagnetic wave into a surface wave which results in increased directivity.

Villeneuve, Behnke, and Kummer of Hughes Aircraft [3] attempted to increase the coverage of an eight element aperture array with all elements excited by narrowing the beamwidth at low beam steering angles. They used

a surface wave structure which consisted of 5 layers of 8-mil thick glass tape. A narrower beam and higher pattern level was realized in the $\theta = 0$ direction, while almost no change resulted in the pattern in the $\theta = 90°$ direction. Their results were obtained experimentally.

Further work should continue into establishing a theoretical explanation of the surface wave effects which improve the directivity for a reactive loaded aperture array at low beam steering angles, and to investigate two dimensional arrays similar to the linear array studied here.

PART TWO

COMPUTER PROGRAM

I. INTRODUCTION

The required subroutines used to generate the figures in this report are included in two previous reports, with the exception of the subroutine which generates the half-space admittance matrix for a wide aperture antenna array which is described and listed in this report. Report [1] contains a description and listing of the subroutines SICI, PATHSP, MAXGCV, MAXGRV, LINER, BLOADC, BLOADR, FUNCTA, FUNCTB, LINEC, EIGEN, and the calling MAIN program, while report [4] contains a description and listing of a univariate optimization program. (Note that other optimization programs could be used to find the reactive loads required for maximum gain.)

II. HALF-SPACE ADMITTANCE MATRIX

The subroutine YHSPA (N, N1, W,L,T,YHS) computes and stores columnwise in YHS the elements of the admittance matrix

$$Y_{ij}^{hs} = \frac{4w}{\eta^2 Lp^2} \sum_{q=1}^{p} \sum_{r=1}^{p} Z_{(iq)(jr)} \tag{1}$$

where

$$Z_{(iq)(jr)} = \frac{\eta}{4\pi} \left[2\,Ci(kx_{(iq)(jr)}) - Ci(u_2) - Ci(v_2)\right]$$

$$- \frac{j\eta}{4\pi} \left[2Si(kx_{(iq)(jr)}) - Si(u_2) - Si(v_2)\right]$$

$$u_2 = k\left(\sqrt{x^2_{(iq)(jr)} + L^2} + L\right)$$

$$v_2 = k\left(\sqrt{x^2_{(iq)(jr)} + L^2} - L\right)$$

$$Ci(x) = -\int_{x}^{\infty} \frac{\cos v}{v}\, dv$$

$$Ci(x) = \int_{0}^{x} \frac{\sin v}{v}\, dv$$

L is the length of the aperture in wavelengths

$x_{(iq)(jr)}$ is the separation distance between the ith aperture q-current strip center and the jth aperture r-current strip center. When i = j and q = r, $x_{(iq)(jr)} = (w/p)/4$.

The following is a list of the abbreviations used in the subroutine calling statement:

N is the number of apertures in the antenna array.

N1 is the number of magnetic current strips per aperture.

W is the width of the aperture (inner waveguide dimension) in wavelengths.

L is the length of the aperture (inner waveguide dimension) in wavelengths.

T is the wall thickness of the waveguide used in wavelengths.

YHS is the storage location for the resulting half-space admittance matrix.

DO loop 10 generates the $x_{(iq)(jr)}$ distances between the centers of all the magnetic current strips of the aperture array. DO loop 11 evaluates on the distinct $Y^{hs}_{(iq)(jr)}$ terms needed to generate the Y^{hs}_{ij} terms - there are 2*N*N1-N-N1+1 distinct terms. DO loop 15 evaluates Eq. (1) using the appropriate weighting coefficients for each $Y^{hs}_{(iq)(jr)}$ term. DO loops 24 and 25 use the upper triangular terms of the symmetric admittance matrix $[Y^{hs}]$ to generate the lower triangular terms.

Minimum allocations are given by

```
COMPLEX YHS(N*N), YHS1(2*N*N1-N-N1+1)
DIMENSION X(N*N1)
```

III. PROGRAM LISTING

```
      SUBROUTINE YHSPA(N,N1,W,L,T,YHS)
      COMPLEX YHS(49),YHS1(72),U
      DIMENSION X(42)
      REAL L,L1
  100 FORMAT(/3X,'X'//(3X,6F7.3))
  101 FORMAT(/2X,' Y - - HALF SPACE'//(3X,5E14.7))
      PI=3.141593
      PI2=2.*PI
      ETA=376.730
      L=L/2.
      L1=L*2.*PI
      Q=2.
      U=(0.,1.)
      L2=L1*L1
      N2=N*N1
      N3=2*N*N1-N-N1+1
      N4=N1+1
      N5=N2+1
      N6=2*N1-1
      N7=N-1
      W1=W/N1
      TL=Q*L1
      TL2=TL*TL
      CS=COS(L1)
      SN=SIN(L1)
      C1=W/(PI*ETA*L*SN*SN*N1*N1)
      C2=SN*CS
      C3=.5*COS(TL)
      X(1)=0.
      IF(N.EQ.1) GO TO 9
      XA=W1*PI2
      DO 10 I=2,N2
      X(I)=(I-1)*XA+(((I-1)/N1)*2.*T)*PI2
   10 CONTINUE
    9 CONTINUE
      WRITE(3,100) (X(I),I=1,N2)
      I1=1
      DO 11 I=1,N3
      IF(I.EQ.1) GO TO 12
      IF(I.GT.N2) GO TO 13
      D2=X(I)*X(I)
      D=SQRT(D2)
      GO TO 14
   12 D=(W1*2.*PI)/4.
      D2=D*D
      GO TO 14
   13 I2=(I-N5)/N7+2
      XJ=X(I1)-X(I2)
      D2=XJ*XJ
      D=SQRT(D2)
      I1=I1+N1
   14 S1=SQRT(D2+L2)
      S2=SQRT(D2+TL2)
      V1=S1+L1
```

```
      U1=D2/V1
      U2=S2+TL
      V2=D2/U2
      CALL SICI(SD,CD,D)
      CALL SICI(SU1,CU1,U1)
      CALL SICI(SV1,CV1,V1)
      CALL SICI(SU2,CU2,U2)
      CALL SICI(SV2,CV2,V2)
      YHS2=C1*(C2*(SU2-SV2-Q*(SV1-SU1))-C3*(Q*(CU1-CD+CV1)-CU2-CV2)-CU1+
     1Q*CD-CV1)
      YHS3=C1*(C2*(CV2-CU2+Q*(CV1-CU1))-C3*(Q*(SU1-SD+SV1)-SU2-SV2)-SU1+
     1Q*SD-SV1)
      YHS1(I)=YHS2-U*YHS3
      IF(I.EQ.N2) I1=N4
      IF(I1.EQ.N5) I1=N4
   11 CONTINUE
      WRITE(3,101) (YHS1(I),I=1,N3)
      DO 15 I=1,N
      I1=(I-1)*N+1
      YHS(I1)=(0.,0.)
      IF(I.GT.1) GO TO 16
      J1=N1
      DO 17 J=1,N1
      IF(J.EQ.N1) GO TO 18
      YHS(1)=YHS(1)+J*2.*YHS1(J1)
      GO TO 19
   18 YHS(1)=YHS(1)+N1*YHS1(J1)
   19 J1=J1-1
   17 CONTINUE
      GO TO 15
   16 J1=I*N1
      J2=N3-N+I
      DO 20 J=1,N6
      IF(J.GT.N1) GO TO 21
      YHS(I1)=YHS(I1)+J*YHS1(J1)
      GO TO 22
   21 YHS(I1)=YHS(I1)+(J-N1)*YHS1(J2)
      J2=J2-N7
   22 J1=J1-1
   20 CONTINUE
   15 CONTINUE
      IF(N.EQ.1) GO TO 23
      DO 24 I=2,N
      I1=I
      DO 25 J=1,N
      J1=N*IABS(I-J)+1
      YHS(I1)=YHS(J1)
      I1=I1+N
   25 CONTINUE
   24 CONTINUE
   23 CONTINUE
      RETURN
      END
```

REFERENCES

[1] J. Luzwick and R. F. Harrington, "A Reactively Loaded Aperture Antenna Array," Tech. Rept. No. 3, Contract No. N00014-76-C-0225, Office of Naval Research, September 1976.

[2] R. F. Harrington and J. R. Mautz, "A Generalized Formulation for Aperture Problems," Scientific Report No. 8, Contract No. F19628-73-C-0047, A. F. Cambridge Research Laboratories, Report AFCRL-TR-75-0589, November 1975.

[3] A. T. Villeneuve, M. C. Behnke, and W. H. Kummer, "Hemispherically Scanned Arrays," Hughes Aircraft Company, Scientific Report No. 2, Contract No. F19628-72-C-0145, A. F. Cambridge Research Laboratories Report AFCRL-TR-74-0084, December 1973.

[4] R. F. Harrington, R. F. Wallenberg, and A. R. Harvey, "Design of Reactively Controlled Antenna Arrays," Tech. Rept. No. 4, Contract No. N00014-67-A-0378-0006, Office of Naval Research, September 1975.

Jan 1974

DISTRIBUTION LIST FOR ONR ELECTRONICS PROGRAM OFFICE

Director
Advanced Research Projects Agency
Attn: Technical Library
1400 Wilson Boulevard
Arlington, Virginia 22209

Office of Naval Research
Electronics Program Office (Code 427)
800 North Quincy Street
Arlington, Virginia 22217

Office of Naval Research
Code 105
800 North Quincy Street
Arlington, Virginia 22217

Naval Research Laboratory
Department of the Navy
Attn: Code 2627
Washington, D. C. 20375

Office of the Director of Defense
Research and Engineering
Information Office Library Branch
The Pentagon
Washington, D. C. 20301

U. S. Army Research Office
Box CM, Duke Station
Durham, North Carolina 27706

Defense Documentation Center
Cameron Station
Alexandria, Virginia 22314

Director National Bureau of Standards
Attn: Technical Library
Washington, D. C. 20234

Commanding Officer
Office of Naval Research Branch Office
536 South Clark Street
Chicago, Illinois 60605

San Francisco Area Office
Office of Naval Research
50 Fell Street
San Francisco, California 94102

Air Force Office of Scientific Research
Department of the Air Force
Washington, D. C. 20333

Commanding Officer
Office of Naval Research Branch Office
1030 East Green Street
Pasadena, California 91101

Commanding Officer
Office of Naval Research Branch Office
495 Summer Street
Boston, Massachusetts 02210

Director
U. S. Army Engineering Research
and Development Laboratories
Fort Belvoir, Virginia 22060
Attn: Technical Documents Center

ODDR&E Advisory Group on Electron Devices
201 Varick Street
New York, New York 10014

New York Area Office
Office of Naval Research
207 West 24th Street
New York, New York 10011

Air Force Weapons Laboratory
Technical Library
Kirtland Air Force Base
Albuquerque, New Mexico 87117

Air Force Avionics Laboratory
Air Force Systems Command
Technical Library
Wright-Patterson Air Force Base
Dayton, Ohio 45433

Air Force Cambridge Research Laboratory
L. G. Hanscom Field
Technical Library
Cambridge, Massachusetts 02138

Harry Diamond Laboratories
Technical Library
Connecticut Avenue at Van Ness, N. W.
Washington, D. C. 20438

Naval Air Development Center
Attn: Technical Library
Johnsville
Warminster, Pennsylvania 18974

Naval Weapons Center
Technical Library (Code 753)
China Lake, California 93555

Naval Training Device Center
Technical Library
Orlando, Florida 22813

Naval Research Laboratory
Underwater Sound Reference Division
Technical Library
P. O. Box 8337
Orlando, Florida 32806

Navy Underwater Sound Laboratory
Technical Library
Fort Trumbull
New London, Connecticut 06320

Commandant, Marine Corps
Scientific Advisor (Code AX)
Washington, D. C. 20380

Naval Ordnance Station
Technical Library
Indian Head, Maryland 20640

Naval Ship Engineering Center
Philadelphia Division
Technical Library
Philadelphia, Pennsylvania 19112

Naval Postgraduate School
Technical Library (Code 0212)
Monterey, California 93940

Naval Missile Center
Technical Library (Code 5632.2)
Point Mugu, California 93010

Naval Ordnance Station
Technical Library
Louisville, Kentucky 40214

Naval Oceanographic Office
Technical Library (Code 1640)
Suitland, Maryland 20390

Naval Explosive Ordnance Disposal Facility
Technical Library
Indian Head, Maryland 20640

Naval Electronics Laboratory Center
Technical Library
San Diego, California 92152

Naval Undersea Warfare Center
Technical Library
3202 East Foothill Boulevard
Pasadena, California 91107

Naval Weapons Laboratory
Technical Library
Dahlgren, Virginia 22448

Naval Ship Research and Development Center
Central Library (Code L42 and L43)
Washington, D. C. 20007

Naval Ordnance Laboratory White Oak
Technical Library
Silver Spring, Maryland 20910

Naval Avionics Facility
Technical Library
Indianapolis, Indiana 46218